Published by :
http://www.ijert.org

International Journal of Engineering Research & Technology (IJERT)
ISSN: 2278-0181
Vol. 13 Issue 10, October 2024

Modeling and Simulation of Energy Management Techniques for Fuel-Cell Based Electric System

Chittoor Dheeraj Krishna Yadav
M-Tech Student,
Dept. of EEE
S V UNIVERSITY, Tirupati

Dr. J.N. Chandra Sekhar,
Associate Professor,
Dept. of EEE
S V UNIVERSITY, Tirupati

Abstract
This work involves conducting a comparative study of various energy management techniques for a fuel-cell-based electric system powering an AC electrical load. The power system under consideration includes supercapacitors, lithium-ion batteries, and fuel cells, alongside relevant DC/AC and DC/DC converters. The energy management techniques examined are widely employed in fuel-cell vehicle submissions and encompass the following: SMCT, the classical proportional–integral control technique, Equivalent consumption minimization technique. Additionally, a simulation model is considered to validate all analyses and performances.

***Keywords*— Battery, supercapacitors, hybridization, energy management, fuel cells, optimization, dc-dc converters.**

I. INTRODUCTION

In recent years, the transportation sector's focus on sustainable energy solutions has led to the expansion of fuel-cell technology, making it a viable option for vehicles. Currently, fuel cells are being utilized in electric vehicles [1], offering a highly efficient, quiet, and eco-friendly alternative to traditional internal combustion engines, with significantly reduced emissions.

Fuel cells must be united with novel energy storage technology, such as supercapacitors or lithium-ion batteries, in order to rise the dynamics and power density of fuel-cell systems. Because some of the load is provided by the batteries and supercapacitors, this hybridization aids the fuel-cell system to be adjusted for upgraded performance and fuel economy. An energy management strategy (EMS) optimizes performance by distributing the load power among various energy sources. Such an EMS should be planned to ensure that every energy source is used within its limitations and to achieve the best possible fuel efficiency. Additionally, the influence of EMS on the hybrid power system's overall life cycle must to be minimized. Various strategies for managing energy have been suggested for fuel cell hybrid systems. One common approach, known as State Machine Control (SMC) Technique, is a rule-based strategy that relies on past experience and heuristics. The effectiveness of SMC depends on the designer's understanding of the system's individual components. A traditional approach to energy management in fuel cell hybrid systems utilizes proportional-integral (PI) controllers to regulate key performance metrics like battery state of charge, supercapacitor voltage, and DC bus voltage [1, 3]. The system's load is distributed to ensure the fuel cell can consistently meet the steady-state power demand. This strategy extends the lifespan of the fuel cell system by mitigating dynamic fluctuations in fuel supply. The fuel cell maintains a relatively steady power output, while other energy sources like batteries charge or discharge to accommodate variations in load. Optimization of fuel cell operation for maximum efficiency or economy, a cost function optimization approach is employed [14, 15]. The equivalent fuel consumption minimization strategy (ECMS) is a popular real-time implementation. It optimizes power distribution by minimizing a real- time cost function that accounts for both fuel cell usage and the equivalent fuel consumption of other energy sources [32].

Most existing energy management strategy (EMS) studies focus on hybrid vehicles, which have regenerative loads with minimal fluctuations compared to aircraft emergency loads. Additionally, these studies often limit their scope to a few EMS techniques and neglect their impact on overall system efficiency and lifespan [22-23, 32]. This paper proposes fuzzy-PI and self-tuning PI-fuzzy hybrid controllers [22]. Previous research has explored intelligent controller methods for three-phase induction motor drives [17] and advanced battery management technologies for optimization [31]. Motivated by these gaps, this paper aims to analyze and comparison of different EMS approaches for a fuel cell hybrid emergency power system (MEA). Key recital metrics include hydrogen consumption, battery and supercapacitor state of charge, overall system efficiency, and component stress.

The energy management techniques executed for comparison are the following:

- ➔ SMC Technique
- ➔ Classical PI Control Technique
- ➔ ECMS

The primary contribution of this work is a verified performance evaluation of typical EMS strategies for an emergency system utilizing fuel cells. The latter is assessed using a novel method that employs the wavelet transform of the instantaneous power of each energy source.

The work is organized as follows. Segment II outlines the hybrid power system's configuration. Segment III discusses component modeling and justification. Segment IV proposed energy management technique. Segment V comparisons of the strategies through simulations and experiments. Finally, the paper concludes with a summary.

Published by :
http://www.ijert.org

International Journal of Engineering Research & Technology (IJERT)
ISSN: 2278-0181
Vol. 13 Issue 10, October 2024

II. HYBRID EMERGENCY POWER SYSTEM CONFIGURATION

The hybrid power system is engineered to meet power and energy needs of an electric vehicle. The fuel-cell system is intended to handle the average demand of 7.5 kW, while the batteries and supercapacitors are meant to support it during periods of continuous and transient peak demand, respectively. [32]

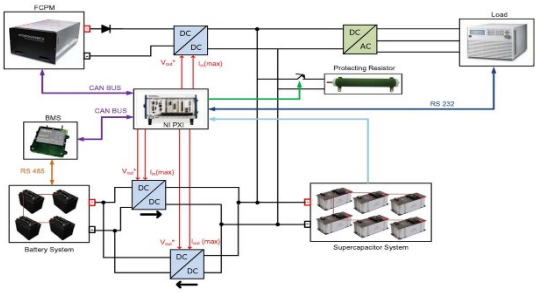

Figure 1: Power System Schematic.

As illustrated in Figure 1, the fuel cell and battery is managed by their individual DC/DC converters, which are overseen by a National Instruments embedded controller (NI PXI-8108).

The main features of the hybrid power system are as follows.

- The fuel cell system is a liquid-cooled PEM fuel cell with power output of 12.5 kW and a voltage range of 60-30 Vdc, featuring integrated auxiliary components.
- The battery system consists of four 12.8 V, 40 Ah lithium-ion battery modules arranged in series.
- The supercapacitor system consists of six 48.6 V, 88 F supercapacitor modules arranged in series.
- The fuel cell DC/DC converter system includes five isolated boost converters, each with a DC input range of 40-64 V and a DC output of 270 V (adjustable between 243-297 V) at 9.2 A, all are arranged in parallel.
- The battery DC/DC converter system comprises two isolated boost converters, each with an input range of 40-58.4 V DC and an output of 270 V DC (adjustable between 243-297 V) at 7 A, connected in parallel. Additionally, it includes a single isolated buck converter with an input range of 243-297 V DC and an output of 48 V DC (adjustable between 0-58.4 V) at a maximum of 20 A.
- The inverter system consists of three isolated DC/AC converters, each with an input range of 160-320 V DC, outputting 200 V AC at 400 Hz and 5 kVA, are arranged in parallel.
- The programmable DC/AC load features six electronically programmable units, each rated at 4.5 kW, 45 A, and 350 V. These units are equipped with digital signal processors, enabling them to simulate both nonlinear and linear AC loads (ranging from 45 to 440 Hz) as well as DC loads.
- Sensors and signal conditioning are installed to measure voltage and current at each converter's input and output.

This section covers the modelling of all these components and provides a more detailed description of each.

III. MODELING OF THE EMERGENCY POWER SYSTEM

In examining energy management techniques, it is necessary t o create a complete and precise model of each central system. this aidsto understand the body's performance and consents the establishment of effective energy management. in this section, displaying of electrical energy in all its aspects is explained.[32]

A. Fuel Cell Model

PEM fuel cells are the most widely used in automotive applications due to their low operating temperatures (≤20°C - ≤100°C). The hybrid system model was developed in MATLAB/Simulink using the Sim Power Systems (SPS) toolbox, which incorporates a fuel cell model. The model includes conduction losses and charging load (resistance and diffusion losses)., the battery output voltage is given by:

$$V = E_{oc} - V_{act} - V_r \qquad (1)$$

Where

$$V_{act} = A \ln\left(\frac{i_{fc}}{i_o}\right) . \frac{1}{sT_d/3+1} \qquad (2)$$

$$V_r = r_{ohm} . i_{fc} \qquad (3)$$

where A is the Tafel slope measured in volts, i_o is the conversation current measured in amperes, r_{ohm} is represents the total resistance from both cell and diffusion measured in ohms, T_d is the battery stabilization time for current step changes.

The output voltage of the fuel cell is determined by the number of cells

$$V_{fc} = N . V \qquad (4)$$

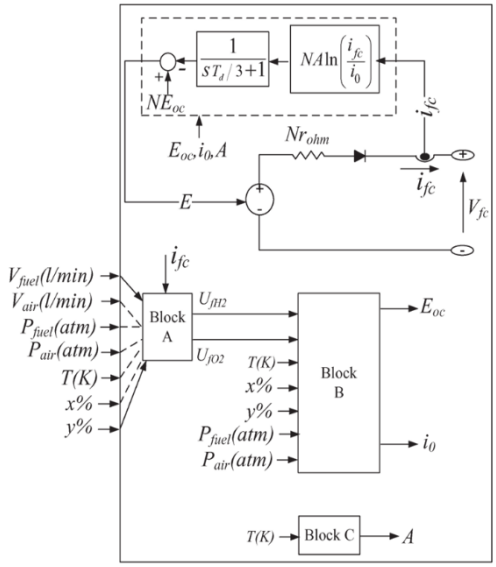

Figure 2: Fuelcell stack model

Figure 2 shows the fuel cell stack model used in SPS.

The essential parameters for the model were gained from the p olarization curve test of FCPM. This allows the performance a nd regularity of the FCPM to be evaluated according to the loa d demand required for the application.

The table 1 displays the parameters necessary for the model

Published by :
http://www.ijert.org

International Journal of Engineering Research & Technology (IJERT)
ISSN: 2278-0181
Vol. 13 Issue 10, October 2024

FUEL CELL INPUT PARAMETERS	Values
Voltage (Vo(v), V1(v))	[52.5, 51.46]
Rated operating point [Inom (A), Vnom (V)]	[250, 43.15]
Maximum operating range [lend (A), Vend (V)]	[320, 39.2]
Number of cells	65
Rated battery pack efficiency (%)	50
Operating temperature (Celcius)	45
Rated Air flow (Ipm)	752
Rated supply pressure [Fuel (bar), Air (bar)]	[1.16, 1]
Rated composition (%) [H2, O2, H2O (Air)]	[99.95, 21, 1]
Fuel cell voltage response time (seconds)	1
Peak O2 utilization (%)	60
Undervoltage (V) @ Peak O2 utilization	2

Table 1: Fuel-cell model input parameters

B. Battery Model

The battery discussed in this article is a lithium-ion battery, as demonstrated in references [16], [18] . This makes them attractive to cars.

The battery model is based on an improved Shepherd curve fitting model, which includes an extra term for voltage polarization to precisely depict the battery's state of charge (SOC) and performance. To ensure analog stability, a battery current filter is employed to regulate the battery current, compensating for polarization resistance.

Similar to the fuel cell model, this model can be easily obtained from data or fundamental dynamic tests.

The primary equations for a Li-ion battery are as follows [26].

The battery voltage is expressed as

$$v_{batt} = E_0 - K\frac{Q}{Q-it}\cdot it - Rb\cdot I + A_b \exp(-B\cdot it) - K\frac{Q}{Q-it}\cdot i* \quad (5)$$

E0 is the battery, where voltage (volts), K is the polarization constant (volts/ampere-hours), Q is the battery capacity (amperes-hours), iâ is the battery filter current (in amps), actual battery capacity (in amps-hours), Ab is the amplitude in the exponential region (in volts), B is the time constant in the exponential region (in Ah) and Rb is the internal energy of the gas light measured in ohms. The time K(Q/(Q−it)) in (5) is called the polarization voltage, though the time K(Q/(Q−it)) is the Polres polarization resistance.

A sudden surge occurs when the battery is fully charged; This behaviour is illustrated by modifying the polarization resistance exclusively during the charging process as follows:

$$Pol_{res} = K\frac{Q}{it-0.1Q} \quad (6)$$

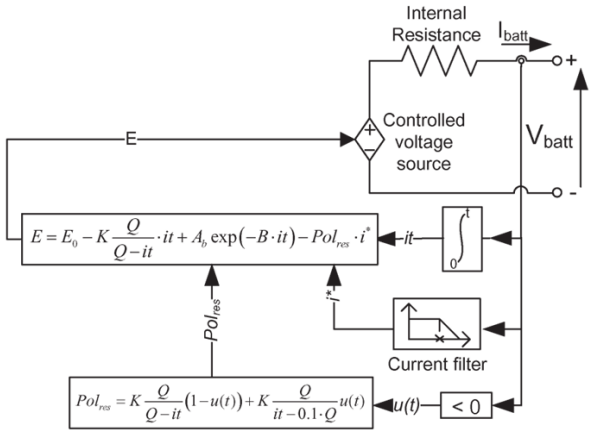

Figure 4: the battery model utilized in SPS.

The experimental setup utilized for obtaining the battery model parameters and for validation purposes is detailed in Table 2.

BATTERY MODEL INPUT PARAMETERS	Values
Rated Voltage (V)	52
Rated Capacity (Ah)	40
Peak Capacity (Ah)	40
Draw Charge Voltage (V)	56.88
Rated output Current (A)	17.4
Internal Resistance (ohm)	0.012
Rated Voltage Capacity (Ah)	36.17
Index field [Voltage (V), Capacity (Ah)]	[57.3 1.96]
Response time battery voltage (sec)	30

Table 2: input parameters for a battery model

B. Supercapacitor Model

It is like electrostatic or electrolytic capacitors, supercapacitors offer the benefit of high capacitance, allowing for greater energy storage and release. [27].

SUPERCAPACITOR MODEL INPUT PARAMETERS	Values
Rated Capacitance (F)	16.6
Equivalent Series Resistance DC (Ohm)	0.15
Rated Voltage (V)	290.6
Ripple Voltage (V)	307
Quantity of Series Capacitance	108
Number of Parallel Capacitors	1
Number of multilayer	6
Molecular Radius (m)	$0.4x10^{-9}$
Operating Temperature (°C)	25

Table 3: Super capacitor input parameters

The supercapacitor model employed in SPS is derived from the Stern model, which combines elements of both the Helmholtz and Gouy-Chapman models.[28].

International Journal of Engineering Research & Technology (IJERT)
ISSN: 2278-0181
Vol. 13 Issue 10, October 2024

The capacitance of the EDLC battery is shown as

$$C = \left[\frac{1}{C_H} + \frac{1}{C_{GC}}\right]^{-1} \quad (7)$$

with

$$C_H = \frac{N_e \varepsilon \varepsilon_0 A_i}{d} \quad (8)$$

$$C_{GC} = \frac{F Q_C}{2 N_e RT} sinh\left(\frac{Q_C}{N_e^2 A_i \sqrt{8RT\varepsilon\varepsilon_0 C}}\right) \quad (9)$$

Where CH and CGC are the Helmholtz and Gouy-Chapman capacitances measured in farads, respectively, ε is the dielectric constant (in farads/meter); Ai is the electrode-electrolyte interface area measured in square meters; d is the Helmholtz layer length (in meters); and Qc represents the value of a single cell. In a supercapacitor segment with Ns cells connected in series and Np cells connected in parallel, the overall capacitance can be calculated as follows:

$$c_T = \frac{N_P}{N_s} \cdot c \quad (10)$$

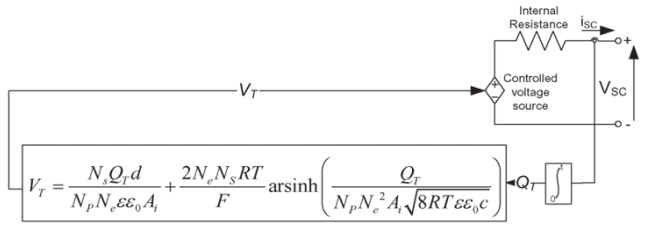

Figure 7: Supercapacitor model

the output voltage of the super capacitor, taking into account the loss, we can use the following formula:

Vout=V cap−Iloss·Req

$$V_{sc} = \frac{Q_T}{c_T} - R_{sc} \cdot i_s c \quad (11)$$

with

$$Q_T = N_P Q_c = \int i_{sc}\, dt \quad (12)$$

Where Q_T is the overall electric charge measured in coulombs, RSC is the supercapacitor segment resistance measured in ohms, and i_{sc} is the supercapacitor segment current measured in amperes. According to equation (7) (8) and (9), CH and CGC represent the Helmholtz capacitance and Gouy capacitance respectively both measured in farads; Ne is the number of electrode layers; ε is the relative dielectric constant (in farads/meter); Ai is the electrode-electrolyte contact area measured in square meters; d is the Helmholtz layer length measured in meters; and Qc is the cell charge for series-connected Ns cells and series-connected Np cells when capacitor modules are connected.

When connected in parallel, the overall capacitance is given as CT = Np Ns × C. (10) Figure 1 shows a typical supercapacitor used in SPS. The model's essential parameters are derived from specifications (measured voltage and current, DC resistance), As the numeral of electrode layers and the molecular radius are fine-tuned for maximum precision. Figure 12 illustrates the supercapacitor's input impedance model and its output curve. Figure 5 compares simulation and test results. Figure 13 illustrates the percentage discrepancy between the simulated and actual output voltages of the supercapacitor system. The model accuracy of approximately ±2% is deemed necessary for the study.

D. DC/DC Converter Model

The Battery system and fuel cell are linked to the DC/AC converter through DC/DC converters, allowing for voltage conversion with accurate regulation of the fuel cell/battery current and the DC bus voltage.

The electric battery DC/DC converter is a boost type, while the battery converter combines a step-up DC/DC converter (output) and a step-down DC/DC converter (charge converter). DC/DC converters can be modeled using also a conversion model or an average value model. Switching function design aims and investigates various pulse width modulation schemes in terms of switching harmonics and loss. Simulating changing models can be very time consuming due to the short time required to evaluate each change. To resolve this problem, this work uses the average-cost DC/DC converter model depicted in Figure 8. The control loop is designed to take into account the dynamics of the model. The performance model is shown in Figure 11. As demonstrated, the converter models and their real-world counterparts exhibit highly similar responses to load changes, including overload conditions.

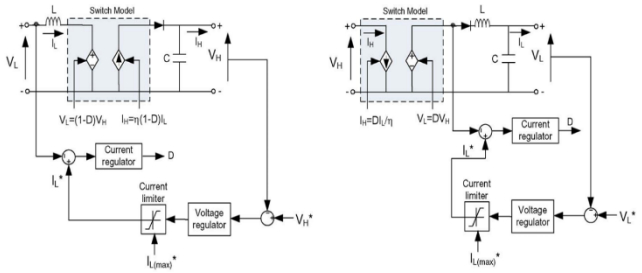

Figure 8 : DC/DC converter model with step up (Boost) & step down Buck

E. DC/AC Converter Model

It is likely the DC/DC converter model, the DC/AC converter model is also embodied using an normal value. A three-phase 200V 400Hz voltage signal was used for the voltage control part. The input current is calculated based on the output voltage and the DC bus voltage.

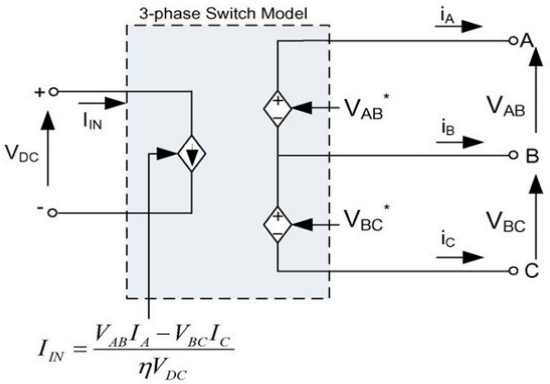

Figure 9: DC/AC Converter model

International Journal of Engineering Research & Technology (IJERT)
ISSN: 2278-0181
Vol. 13 Issue 10, October 2024

F. Emergency Load Model

The load is depicted as a three-phase regulated current source. where the load current is calculated based on the three-phase apparent power (in kVA), the power factor, and the nominal line voltage.

IV. ENERGY MANAGEMENT TECHNIQUES

This is done by using EMS to manage the energy comeback of individual energy and load demand from connected devices. The main difference between EMS controlling all EMS concepts depends on the method of obtaining the fuel. The following sections define EMS.

A. state machine control (SMC) Technique

These states are resulting using the same method as in [8]. The electrical power is resolute by the SOC choice of the battery a nd the electrical power P_{load}.

B. Classical PI Control Technique

This approach customs as a PI controller to regulate battery state of charge (SOC), as illustrated in Figure 10. The electric power is determined by withdrawing the load power from the battery power output of the PI controller. When the battery's state of charge (SOC) surpasses the set threshold, the voltage from the fuel cell drops, and the battery takes over, providing full power. On the other hand, if the SOC drops below the reference level, the fuel cell supplies only a trivial amount of power to the load. This method is more user-friendly than earlier approaches, and it allows for online adjustment of the PI gain to enhance performance.

C. ECMS

ECMS is used value-based approach [14-16]. It aims to minimize fuel consumption by optimizing fuel cell usage and battery state of charge (SOC) management. This paper adopts the model proposed in [16] to regulate battery Equivalent Fuel Consumption Minimization (ECMS) is a widely SOC, incorporating a penalty coefficient for battery power.the process is shown in Figure 13. The optimization challenge is outlined as follows.

Invention of an optional solution $x = [P_{fc}, \alpha, P_{batt}]$, which decreases

$$F = [P_{fc} + \alpha P_{batt}] \cdot \Delta T \qquad (13)$$

Within the framework of equality constraints

$$P_{load} = P_{fc} + P_{batt} \qquad (14)$$

$$\alpha = 1 - 2\mu \frac{(SOC - 0.5(SOC\max + SOC\min))}{SOC\max + SOC\min}$$

Within the boundary conditions

$P_{fc\ min} \leq P_{fc} \leq P_{fc\ max}$

$P_{batt\ min} \leq P_{batt} \leq P_{batt\ max}$

$0 \leq \alpha \leq 100$

where P_{fc}, P_{batt}, and P_{load} are the load power, battery power, and fuel-cell power (including transformer) respectively. α is the charge coefficient, and μ is a continual (changed to 0.6 to better control the battery SOC). ΔT is the sampler time. P_{fcmin} and P_{fcmax} are the minimum and maximum fuel-cell power, respectively. $P_{battmin}$ and $P_{battmax}$ are the minimum and maximum battery-operated capacity with power, respectively. SOC_{min} and SOC_{max} are the minimum and maximum battery SOC respectively.

This means that when the supercapacitor is discharged, it is recharged using the same energy provided by the battery system. Consequently, throughout the load cycle, the fuel cell and the battery exclusively share the entire energy load.

.

V. SIMULATION AND RESULTS

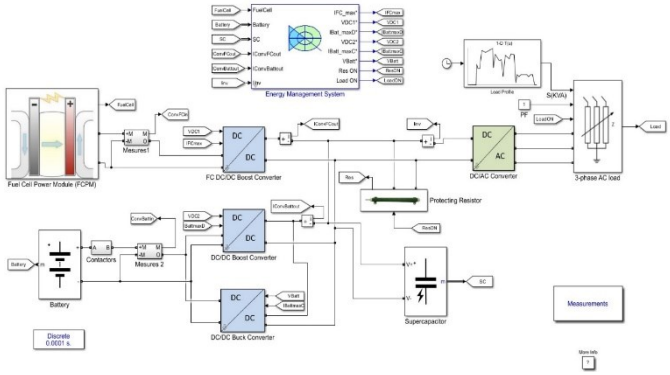

Figure 10: EMS Simulink module

I) State Machine Control (Smc) Technique:

In state machine control (SMC) technique from At T=50 sec, the flowchart shows a load of 4832W, with the fuel cell and battery contributing 2663W and 3220W respectively, while the supercapacitor is absorbing 1044W.

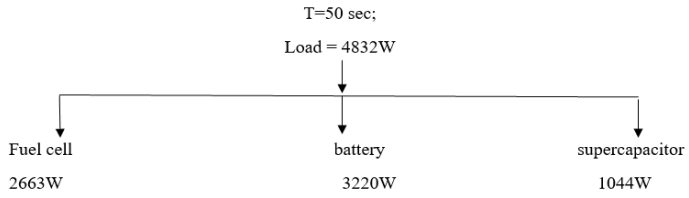

At T = 150 sec, the load is 7940W, with the fuel cell and battery providing 7559W and 3501W respectively, while the supercapacitor is absorbing 3797W.

.

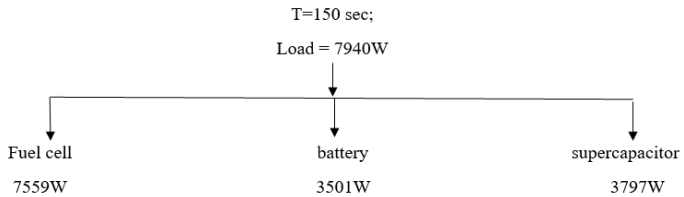

At T= 250 sec, the load is 2919W with the fuel cell and battery providing 4888W & 1373W respectively, while the supercapacitor is absorbing 5883W.

International Journal of Engineering Research & Technology (IJERT)
ISSN: 2278-0181
Vol. 13 Issue 10, October 2024

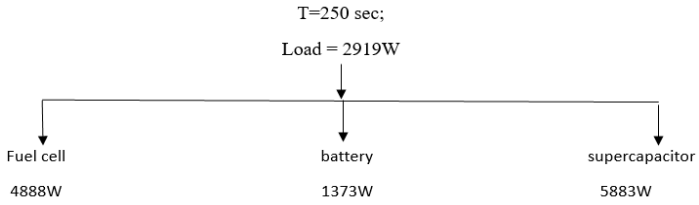

At T= 325 sec, the load is 3423W with the fuel cell and battery providing 3305W & 1551W respectively, while the supercapacitor is absorbing 2975W.

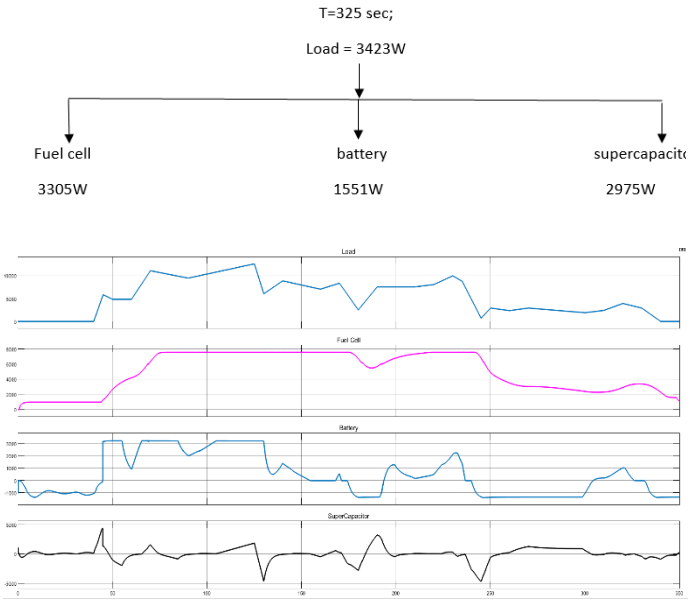

Figure 11: Power dividing between Load, fuel cell, Battery, Supercapacitor for AC load in state machine control technique

II. Classical Pi Control Technique:

In Classical PI Control Strategy at T= 50 sec, the load is 4832W with the fuel cell and battery providing 1701W & 3220W respectively and supercapacitor is absorbing 8149W.

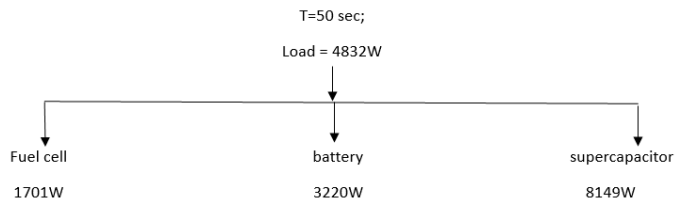

At T= 150 sec, the load is 7899W with the fuel cell and battery providing 7506W & 3208W respectively and supercapacitor is absorbing 2808W.

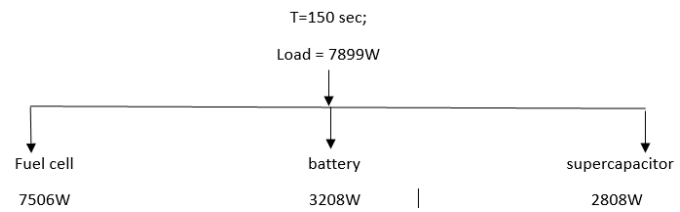

At T= 250 sec the load is 2912W with the fuel cell and battery providing 4032W & 1377W respectively and supercapacitor is absorbing 2651W.

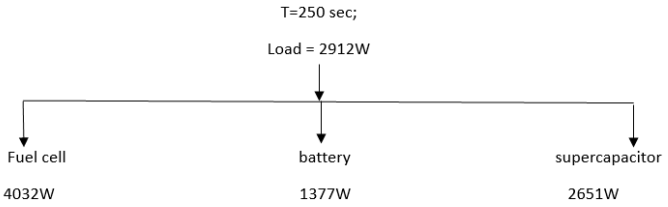

At T= 325 sec the load is 3395W with the fuel cell and battery providing 2941W & 1353W respectively and supercapacitor is absorbing 1815W.

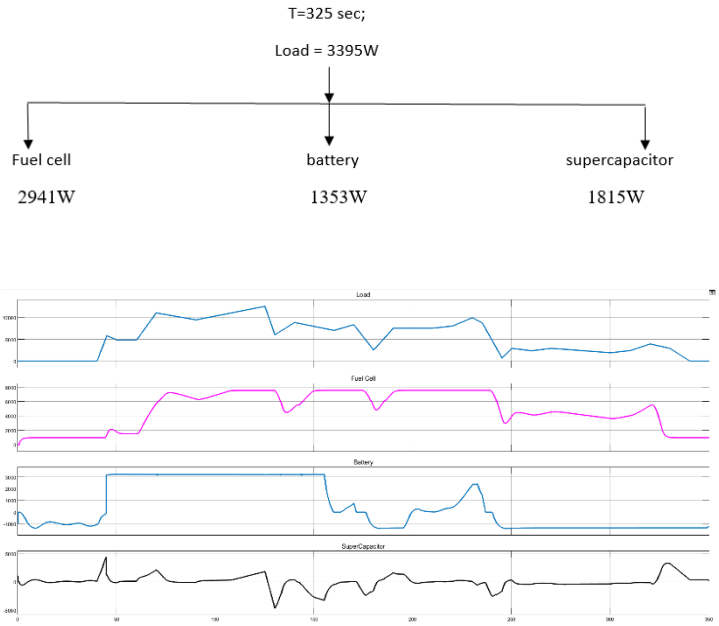

Figure 12: Power dividing between Load, fuel cell, Battery, Supercapacitor for AC load in Classical PI Control technique

III. Equivalent Consumption Minimization Strategy:

In Equivalent Consumption Minimization Strategy at T= 50 sec, the load is 4832W with the fuel cell and battery providing 5956W & 9651W respectively and supercapacitor is absorbing 1020W.

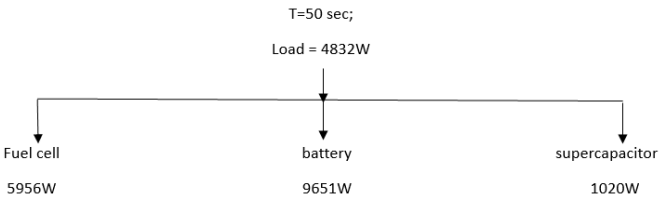

At T= 150 sec, the load is 7953W with the fuel cell and battery providing 7556W & 3670W respectively and supercapacitor is absorbing 3701W.

International Journal of Engineering Research & Technology (IJERT)
ISSN: 2278-0181
Vol. 13 Issue 10, October 2024

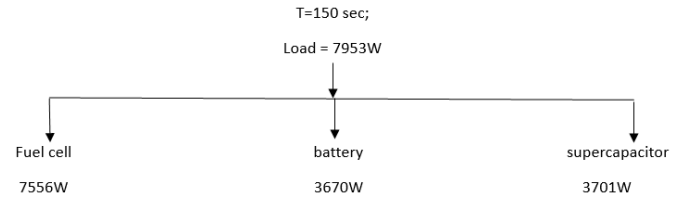

At T= 250 sec, the load is 2919W with the fuel cell and battery providing 3974W & 1368W respectively and supercapacitor is absorbing 3209W.

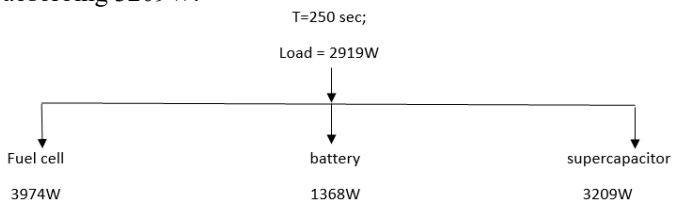

At T= 325 sec, the load is 3423W with the fuel cell and battery providing 5338W & 1342W respectively and supercapacitor is absorbing 5654W.

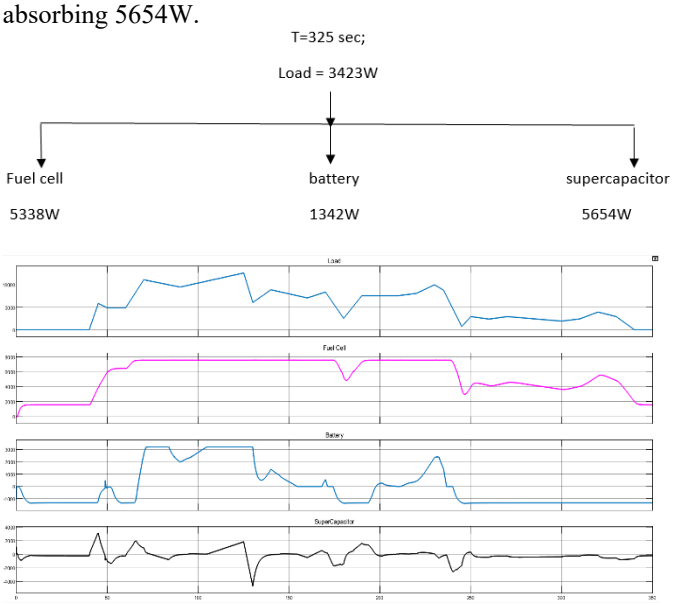

Figure 13: Power dividing between Load, fuel cell, Battery, Supercapacitor for AC load in Equivalent consumption minimization strategy

CONCLUSION

Among the examined strategies, ECMS stands out as an effective approach for fuel-cell-based power systems. It reduces hydrogen consumption, improves overall efficiency, and ensures stable operation. ECMS to develop the performance of energy management systems in fuel-cell vehicles.

REFERENCES

[1] P. Thounthong and S. Rael, "The benefits of hybridization," IEEE Ind. Electron. Mag., vol. 3, no. 3, pp. 25–37, Sep. 2009.
[2] P. Thounthong, S. Rael, and B. Davat, "Control strategy of fuel cell and supercapacitors association for a distributed generation system," IEEE Trans. Ind. Electron., vol. 54, no. 6, pp. 3225–3233, Dec. 2007.
[3] Z. Amjadi and S. Williamson, "Power-electronics-based solutions for plug-in hybrid electric vehicle energy storage and management systems," IEEE Trans. Ind. Electron., vol. 57, no. 2, pp. 608–616, Feb. 2010.
[4] G. Renouard-Vallet, M. Saballus, G. Schmithals, J. Schirmer, J. Kallo, and A. K. Friedrich, "Improving the environmental impact of civil aircraft by fuel cell technology: Concepts and technological progress," Energy Environ. Sci., vol. 3, no. 10, pp. 1458–1468, 2010.
[5] G. Renouard -Vallet, M. Saballus, G. Schmithals, J. Schirmer, J. Kallo, and A. K. Friedrich, "Fuel cells for aircraft applications," ECS Trans., vol. 30, no. 1, pp. 271–280, 2011.
[6] X.Roboam, B.Sareni, and A.D.Andrade, "More electricity in the air: To ward optimized electrical networks embedded in more-electrical aircraft," IEEE Ind. Electron. Mag., vol. 6, no. 4, pp. 6–17, Dec. 2012.
[7] W. Jiang and B. Fahimi, "Active current sharing and source management in fuel cell-battery hybrid power system," IEEE Trans. Ind. Electron., vol. 57, no. 2, pp. 752–761, Feb. 2010.
[8] P. Garcia, L. M. Fernandez, C. A. Garcia, and F. Jurado, "Energy management system of fuel-cell-battery hybrid tramway," IEEE Trans. Ind. Electron., vol. 57, no. 12, pp. 4013–4023, Dec. 2010.
[9]J- Ke, R.Xinbo, Y. Mengxiong, and X.Min, "A hybrid fuel cell power system," IEEE Trans.Ind.Electron., vol. 56, no. 4, pp. 1212–1222, Apr. 2009.
[10] S. Caux, W. Hankache, M. Fadel, and D. Hissel, "On-line fuzzy energy management for hybrid fuel cell systems," Int. J. Hydrogen Energy, vol. 35, no. 5, pp. 2134–2143, Mar. 2010.
[11] L. Chun-Yan and L. Guo-Ping, "Optimal fuzzy power control and man agement of fuel cell/battery hybrid vehicles," J. Power Sources, vol. 192, no. 2, pp. 525–533, Jul. 15, 2009.
[12] X. Zhang, M. C. Chunting, A. Masrur, and D. Daniszewski, "Wavelet transform-based power management of hybrid vehicles with multiple on board energy sources including fuel cell, battery and ultracapacitor," J. Power Sources, vol. 185, no. 2, pp. 1533–1543, Dec. 1, 2008.
[13] B. Vural, A. R. Boynuegri, I. Nakir, O. Erdinc, A. Balikci, M. Uzunoglu, H. Gorgun, and S. Dusmez, "Fuel cell and ultra-capacitor hybridization: A prototype test bench based analysis of different energy management strategies for vehicular applications," Int. J. Hydrogen Energy, vol. 35, no. 20, pp. 11161–11171, Oct. 2010.
[14] P. Rodatz, G. Paganelli, A. Sciarretta, and L. Guzzella, "Optimal power management of an experimental fuel cell/supercapacitor-powered hybrid vehicle," Control Eng. Pract., vol. 13, no. 1, pp. 41–53, Jan. 2005.
[15] L. Xu, J. Hua, J. Li, and M. Ouyang, "Distributed control system based on CAN bus for fuel cell/battery hybrid vehicle," in Proc. IEEE ISIE, Jul. 5–8, 2009, pp. 183–188.
[16] P. Garcia, J. P. Torreglosa, L. M. Fernandez, and F. Jurado, "Viability study of a FC-battery-SC tramway controlled by equivalent consumption minimization strategy," Int. J. Hydrogen Energy, vol. 37, no. 11, pp. 9368 9382, Jun. 2012.
[17] D Nikhitha, JNC Sekhar, "Modeling and simulation of IM drive performance using PI, ANN and FLC,"- 2013 International Conference on IT Convergence and …, 2013.
[18] F. Savoye, P. Venet, M. Millet, and J. Groot, "Impact of periodic current pulses on li-ion battery performance," IEEE Trans. Ind. Electron., vol. 59, no. 9, pp. 3481–3488, Sep. 2012.
[19] W. Greenwell and A. Vahidi, "Predictive control of voltage and current in a fuel cell-ultracapacitor hybrid," IEEE Trans. Ind. Electron., vol. 57, no. 6, pp. 1954–1963, Jun. 2010. [20] K. Min-Joong and P. Huei, "Power management and design optimization of fuel cell/battery hybrid vehicles," J. Power Sources, vol. 165, no. 2, pp. 819–832, Mar. 20, 2007.
[21] J. Moreno, M. E. Ortuzar, and J. W. Dixon, "Energy-management system for a hybrid electric vehicle, using ultracapacitors and neural networks," IEEE Trans. Ind. Electron., vol. 53, no. 2, pp. 614–623, Apr. 2006.
[22] S Pravallika, JNC Sekhar, DP Reddy, "Optimization of speed control of induction motor using self -tunned PI plus fuzzy hybrid controller," Int J Emerg Technol Adv Eng, 2015.
[23] W. S. Lin and C. H Zheng, "Energy management of a fuel cell/ ultracapacitor hybrid power system using an adaptive optimal-control method," J. Power Sources, vol. 196, no. 6, pp. 3280–3289, Mar. 15, 2011.
[24] P. Pisu and G.Rizzoni, "A comparative study of supervisory control strate gies for hybrid electric vehicles," IEEE Trans. Control Syst. Technol., vol. 15, no. 3, pp. 506–518, May 2007.
[25] A. Fadel and B. Zhou, "An experimental and analytical comparison study of power management methodologies of fuel cell-battery hybrid vehicles," J. Power Sources, vol. 196, no. 6, pp. 3271–3279, Mar. 15, 2011.
[26] J. Padulles, G. W. Ault, and J. R. McDonald, "An integrated SOFC plant dynamic model for power systems simulation," J. Power Sources, vol. 86, no. 1/2, pp. 495–500, Mar. 2000.
[27] S. M. Njoya, O. Tremblay, and L.-A. Dessaint, "A generic fuel cell model for the simulation of fuel cell vehicles," in Proc. IEEE VPPC, Sep. 7–10, 2009, pp. 1722–1729.
[28] O. Tremblay, L.-A. Dessaint, and A.-I. Dekkiche, "A generic battery model for the dynamic simulation of hybrid electric vehicles," in Proc. IEEE VPPC, Sep. 9–12, 2007, pp. 284–289.

International Journal of Engineering Research & Technology (IJERT)
ISSN: 2278-0181
Vol. 13 Issue 10, October 2024

[29] V. Musolino, L. Piegari, and E. Tironi, “New full-frequency-range supercapacitor model with easy identification procedure,” IEEE Trans. Ind. Electron., vol. 60, no. 1, pp. 112–120, Jan 2013.
[30] K. B. Oldham, “A Gouy–Chapman–Stern model of the double layer at a (metal)/(ionic liquid) interface,” J. Electroanal. Chem., vol. 613, no. 2, pp. 131–138, Feb. 2008.
[31] SH Chandra, JN ChandraSekhar, “Battery Management Systems for Electric Vehicles Using Lithium-Ion Batteries,” - International Journal of Science and Research, 2022
[32] S Souleman Njoya Motapon, Louis-A. Dessaint, Kamal Al-Haddad. "A Comparative Study of Energy Management Schemes for a Fuel-Cell Hybrid Emergency Power System of More-Electric Aircraft", IEEE Transactions on Industrial Electronics, 2014.